Anisotropic emission of neutral atoms: evidence of an anisotropic Rydberg sheath in nanoplasma

2015 New J. Phys. 17 023033

(http://iopscience.iop.org/1367-2630/17/2/023033)

IOP Publishing New J. Phys. 17 (2015) 023033 doi:10.1088/1367-2630/17/2/023033

New Journal of Physics
The open access journal at the forefront of physics

Deutsche Physikalische Gesellschaft DPG
IOP Institute of Physics

Published in partnership with: Deutsche Physikalische Gesellschaft and the Institute of Physics

OPEN ACCESS

RECEIVED
3 August 2014

REVISED
4 December 2014

ACCEPTED FOR PUBLICATION
12 January 2015

PUBLISHED
10 February 2015

PAPER

Anisotropic emission of neutral atoms: evidence of an anisotropic Rydberg sheath in nanoplasma

R Rajeev, T Madhu Trivikram, K P M Rishad and M Krishnamurthy

Tata Institute of Fundamental Research, Homi Bhabha Road, Mumbai, 400 005, India

E-mail: mkrism@tifr.res.in

Keywords: clusters, intense lasers, acceleration

Abstract

Intense laser-produced plasma is a complex amalgam of ions, electrons and atoms both in ground and excited states. Little is known about the spatial composition of the excited states that are an integral part of most gaseous or cluster plasma. In cluster-plasma, Rydberg excitations change the charge composition of the ions through charge transfer reactions and shape the angular distributions. Here, we demonstrate a non-invasive technique that reveals the anisotropic Rydberg excited cluster sheath by measuring anisotropy in fast neutral atoms. The sheath is stronger in the direction of light polarization and the enhanced charge transfer by the excited clusters results in larger neutralization.

1. Introduction

Intense laser plasma studies have found methods for compact electron, [1, 2] positron, [3] and ion acceleration [4] with 10,000 times larger field gradients than conventional accelerators. The key feature is the ability to convert oscillating electric fields of light to short lived electrostatic fields. In solid targets, a substantial density of electrons leaves the solid slab instantly, generates a strong electrostatic field and drives the ions normal to the target [5]. In nano-clusters, where the particle size is much smaller that the light wavelength, intra-cluster density of a solid leads to a very strong ionization [6–8]. A mean charge as large as 8+ has been demonstrated with Argon clusters even at modest intensities of 10^{16}W cm^{-2}[9]. Such high charge density leads to strong Coulomb explosion leading to MeV ion energies. Hydrodynamics plasma heating and ion acceleration is also envisaged for larger clusters with a few million atoms [10].

In low density gas experiments, as electrons respond instantly, appropriately tailored wake fields [11, 12] generate a directed beam of even GeV electrons [13]. Directed ion acceleration is far more difficult [14]. Since ion motion takes longer than the light pulse duration, the environment surrounding the laser plasma plays a crucial role. In a dense ensemble of atoms/clusters exposed to a short burst of $\simeq$100 eV electrons, electronic excitation is as important as ionization [15]. While effects like non-local ionization in the surrounding media have been studied for better understanding of the shock waves, the role of excitation has largely been ignored [16]. Given that there can be substantial energy transport in excitation, it will be crucial to understand the role of excited states in general in any hot dense plasma.

A Rydberg excited system interacts very differently to a normal atom/cluster. Their ionization energy is small, the electron orbits are larger and these features change the nature of the interaction. For example, charge transfer cross section can be larger [17] by 10^4. Appropriate use of these resulted in a novel scheme for neutral atom acceleration [15]. These studies demonstrated the phenomenon that, in a dense cluster ensemble, electrons released from the clusters in a focal volume collision excite clusters surrounding the focal volume and form a Rydberg excited sheath. Enhanced charge transfer from the Rydberg excited clusters (ECTREC) leads to neutral atom generation. Probing microscopic variations of the excitation sheath which spans 100–200μm space around the focal volume and lasts a few picoseconds is a non-trivial pursuit but vital to understanding the hot dense plasma evolution. The excitation sheath has a decisive effect on the charge composition of the ions and manipulating it by laser parameters like polarization or pulse duration can bring important changes to neutral

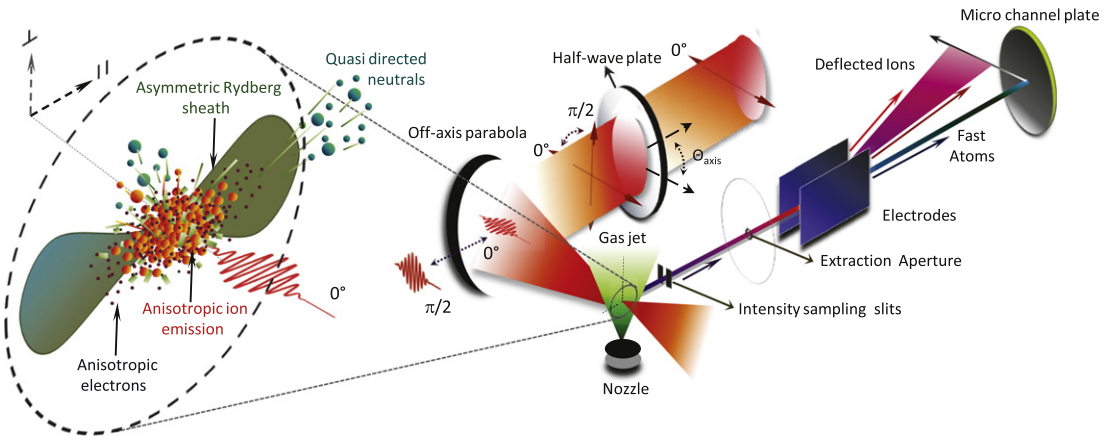

Figure 1. Intense laser pulses are focused using an off-axis parabola near a supersonic jet nozzle to ionize argon clusters to generate fast ions or neutrals that are probed using a TPS. A half wave plate changes the polarization direction and the neutral atom emission is measured when light polarization is aligned towards the detector (horizontal polarization—H) or in the perpendicular direction (vertical polarization—V). Anisotropic electron emission (black dots) generates an anisotropic Rydberg excited cluster sheath surrounding the focus (greenish region) through inelastic collisions. Larger propensity of Rydberg excited clusters along the laser polarization reduces the ion (red spheres) more efficiently to result in anisotropic fast neutral atoms.

atom emission. A more directed emission of fast neutrals is a major leap towards devising applications in the electronics industry and energy research [18, 19].

In ionization of matter, a plane-polarized light preferentially forces electrons along the polarization direction and leads to an anisotropic emission. Electron yield is a few 100 times larger along the polarization [20] in atoms or molecules. In spherical clusters, where collisional and plasma features dominate, it is also a few times larger along the light polarization [21–24]. Anisotropy in electron emission in turn drives the ions to be anisotropic [25–27]. While anisotropic electron and ion emission is observed from single clusters, in a dense cluster ensemble additional polarization dependent dynamics are important due to the presence of a large fraction of Rydberg excited clusters [15]. This has far reaching consequences on the accelerated atom angular distributions, which forms the subject of investigation of this report.

Intense field ionization of nano-clusters dominantly give low energy (<400 eV) electrons [21–23] and in a dense cluster ensemble it is shown that these electrons collisionally excite a substantial fraction of clusters to Rydberg states in the region surrounding the focal volume [15]. Further, it is shown that the sheath of Rydberg excited clusters reduces all the ions Coulomb exploded from the clusters in the focal volume to neutral atoms [15]. If the sheath is symmetric to the laser polarization, the neutral atoms would have the same anisotropy as that of the ions formed in the laser focus, since the charge transfer reactions do not depend on the direction. On the other hand, an enhancement in the anisotropy of the neutral atoms as compared to that of ions would indicate that charge transfer reaction rate is different along different directions. This occurs only if the density of excited clusters is different along different directions or the Rydberg excited cluster sheath is anisotropic. In this paper, we evolve a novel method where neutral atom anisotropy is used to characterize the anisotropy in the sheath. The experiments shown here reveal that the neutral atom emission has a more enhanced anisotropy than fast ions. By computing the neutral atom yield formed in charge transfer collisions with the Rydberg excited clusters and correlating this with the experimental measurements, the anisotropy in the Rydberg excited cluster sheath is inferred. Thus a novel scheme of using charge transfer reactions to probe microscopic variations in the excitation sheath generated in the region surrounding the focal volume is devised.

2. Experiment

Figure 1 shows the experimental schematic, which uses 70 fs long laser pulses centered at 800 nm. The intense laser light is focused using a f/3 off-axis parabolic mirror to achieve an intensity of 7×10^{16} W cm^{-2}. Argon clusters are generated by a supersonic jet pulse valve equipped with a 45° conical nozzle 750 μm in diameter. A backing pressure of about 10 atm is used to generate argon clusters that are expected to have a log normal distribution of sizes with a most probable size of about 7,000. The cluster size is characterized by using the well established procedure of evaluating the Hagena parameter for argon [28, 29] with the physical dimensions of the nozzle used in the experiment. Rayleigh scattering measurements are independently carried out to ensure that the cluster size changes with the backing pressure as expected and the mean size of the clusters is inferred [29, 30]. Using the Wigner–Seitz radius (2.23 Å) for argon and assuming that the nano-particle has the solid

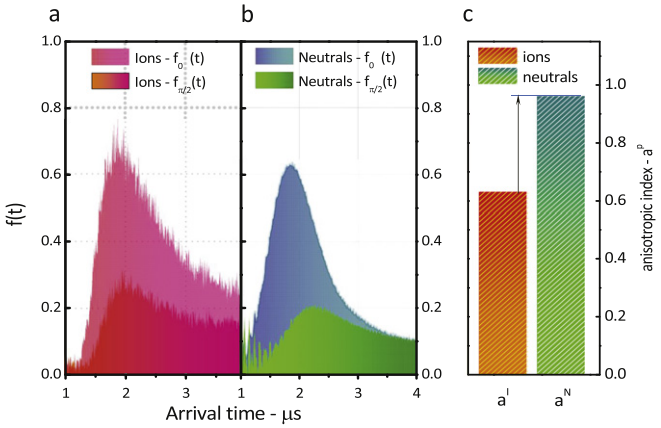

Figure 2. Time-of-flight measurements of (a) energetic ions and (b) fast atoms formed when $Ar_{7,000}$ clusters are ionised at 7×10^{16}W cm^{-2} in directions parallel (0) and perpendicular ($\pi/2$) to the laser polarization. While the ion measurements are made in the single cluster regime [9], the measurements on neutral atoms are made on a dense ensemble [15] under otherwise identical conditions. (c) The mean of the energy dependent anisotropy a^{I} and a^{N} of ions and neutrals, respectively, is depicted as a bar diagram. The enhanced anisotropy of neutral atoms is indicated by the arrow.

density of argon, the average radius of the cluster is estimated to be about 2 nm [31]. The laser pulses are focused a few mm away from the nozzle where the ensemble density is $\sim 1 \times 10^{14}$ cm^{-3}. The pressure in the chamber is maintained at about 10^{-4} Torr with the gas load. Ion or neutral atom measurement is carried out using a Thomson parabola spectrometer that is equipped with a position sensitive microchannel plate detector coupled to a phosphor screen. A CCD camera is used acquire the ion images. A more detailed description of the experiment has recently been published [9].

The neutral atom signal is monitored using the Thompson parabola spectrometer (TPS) [9] where the electric field on the TPS is made large enough to deflect all the ions out of the detector [15]. The time-of-flight (TOF) of the particles measured at the undeflected spot in TPS discriminates the photons (arrival time of a few nanoseconds) and the neutrals (arrival time of $\simeq 1-4$ μs). TOF is thus used to measure the yield and the kinetic energy distribution of the fast atoms. Light polarization is varied with a $\lambda/2$ plate and the TOF signals along the polarization ($f_0(t)$) are compared with those in the perpendicular direction ($f_{\pi/2}(t)$).

The TOF signals (in figure 2(b)) and the associated energy distribution of the neutrals (figure 3(a)) clearly show that for most of the neutral atoms (>10 keV), the emission along the polarization is larger than in the perpendicular direction. The anisotropy in the emission of a particle p (be it ion I or neutral atom N or electron e) of energy E is defined to be

$$A^p(E) = \frac{F_0^p(E) - F_{\pi/2}^p(E)}{\left(F_0^p(E) + F_{\pi/2}^p(E)\right)/2} \quad (1)$$

where $F_0^p(E)$ and $F_{\pi/2}^p(E)$ are the spectral distributions of the particle p along parallel and perpendicular directions to the laser polarization, respectively. For an isotropic distribution, $A^p(E)$ will be close to zero and for a fully anisotropic distribution corresponding to no particle emission along the perpendicular direction $A^p(E)$ assumes a value of 2. $A^p(E) \simeq 1$, implies a three times larger particle flux along the polarization direction.

Given that the neutral atom emission is anisotropic with three times larger yield along the laser polarization (see $A^{\mathrm{N}}(E)$ in figure 3(b)), the first question to answer is if the neutrals are anisotropic only because the ions are anisotropic [25] or is there any additional anisotropy brought out by the multi-cluster ensemble that generates the neutrals. Experiments are carried out to measure the ion anisotropy formed in single cluster ionization by independent measurements, but under otherwise identical conditions. In these measurements, clusters are sampled through a 500 μm conical skimmer in a differentially pumped chamber at $\sim 10^{-7}$ Torr pressure at a lower cluster density $\sim 10^{10}$ clusters cm^{-3}, where ion collisions with background gas are negligible as elaborated in the previous work [15]. Inset of figure 3(a) shows the energy distributions ($F(E)$) of ions (I) from single clusters derived from the arrival signals ($f(t)$) in figure 2(a). Ion flux along the laser polarization is only about 2 times larger than that in the perpendicular direction. The present measurements also show that anisotropy in ions is prevalent at nearly all energies, unlike previous experiments [25], due to a major difference in the experimental geometry. In earlier experiments the ion signal was collected over the entire focal volume, while the present experiments sample the ions only from the high intensity region (200 μm region of the focal volume [9]). The focal volume slicing improvises the TPS resolution [9] and reducing the ion emission angular width is important in anisotropy measurements.

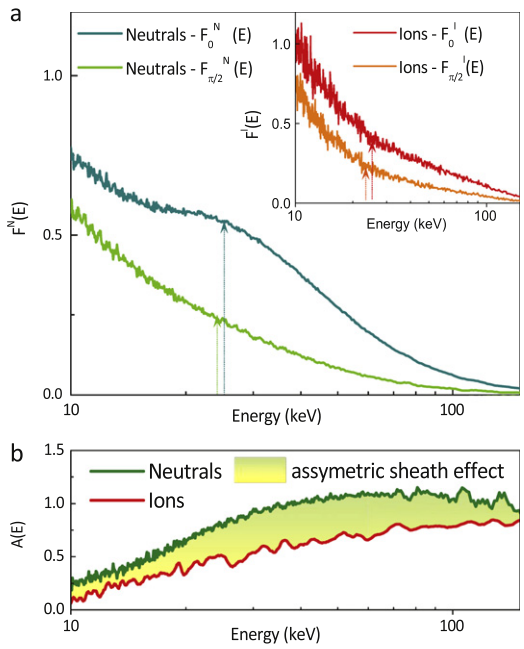

Figure 3. (a) Energy spectrum of neutral atoms and ions (inset) for Ar_{7000} clusters ionized at 7×10^{16}W cm^{-2} show that the particle emission along the parallel (0) direction is larger compared to the perpendicular direction ($\pi/2$) to the laser polarization. Relative length of the arrows indicates that the fast atom yield along the laser polarization is relatively much larger than the ions. (b) The enhanced anisotropy of neutral atom emission (indicated in shading) is shown in the measured anisotropy function $A(E)$ (see equation (1) for definition).

3. Results and discussion

The anisotropic functions given in figure 3(b) for both ions and neutrals show that the neutrals are more anisotropic. Shading in figure 3(b) shows the enhancement in neutral atom anisotropy ($A^{\mathrm{N}}(E) - A^{\mathrm{I}}(E)$). The cluster explosion physics is quite complex and the measured energy spectrum involves averaging over the ions from different shells with different charges states. The experiments are also convoluted with the log-normal distribution of the cluster size and intensity variation over the focal volume [32]. Comprehending the details of the energy spectrum is in itself quite involved and the charge transfer physics adds a more difficult additional complexity to compute the energy dependent anisotropy. A better comparison is offered by a mean of the energy dependent anisotropy distribution a^p for a particle p . The bar plot in figure 2(c) shows the experimentally measured mean anisotropy for ions and neutrals. The plot clearly quantifies the enhancement in neutral atom anisotropy as indicated by the arrow. The neutral yield ratio between the parallel and perpendicular polarizations directions defined as $y^{\mathrm{N}} = Y_0^{\mathrm{N}}/Y_{\pi/2}^{\mathrm{N}}$ is derived from the indices a^{I} and a^{N} as

$$y_{\mathrm{N}} = \frac{\left(1 + a^{\mathrm{N}}/2\right)\left(1 - a^{\mathrm{I}}/2\right)}{\left(1 - a^{\mathrm{N}}/2\right)\left(1 + a^{\mathrm{I}}/2\right)} \tag{2}$$

Here Y_0^{N} and $Y_{\pi/2}^{\mathrm{N}}$ are the respective neutral yields or the fraction of neutral atoms formed from the ions. The neutral atom anisotropy is clearly not just a reflection of the source (ion) anisotropy. If that were the case, $a^{\mathrm{I}} \sim a^{\mathrm{N}}$ and the yield ratio y_{N} would be 1. In the present experiments, $a^{\mathrm{I}} = .6, a^{\mathrm{N}} = .9$ and $y_{\mathrm{N}} \sim 1.5$. Since $y^{\mathrm{N}} > 1$, it implies preferential neutralization along the laser polarization and is a clear indicator of an anisotropic effect in the very process of neutralization. This is feasible only if the density of the Rydberg excited systems encountered by the ion is much larger in the parallel direction or in other words if the sheath of the Rydberg excited clusters is anisotropic.

To validate these conclusions, we further measure the electron anisotropy which is the source of the sheath. Electron energy distributions (figure 4(a)) measured with a repelling potential analyzer [22], at low cluster densities (single cluster interactions), show that the electrons are much more anisotropic as the yield along the polarization direction is much larger. As can be seen from figure 4 (a), the slope of the energy spectrum does not change much and indicates that the electron temperature changes very little with the polarization. The integral electron anisotropy a^e is measured to be $\sim$1.47 which implies an integral flux ratio κ, defined as $\kappa \sim \int F_{\pi/2}^e(E)\,\mathrm{d}E \Big/ \int F_0^e\,\mathrm{d}E$ of about 1/9. A nine times larger electron yield along laser polarization would result in proportionately larger inelastic collision rate that generates a larger fraction of excited clusters or a denser

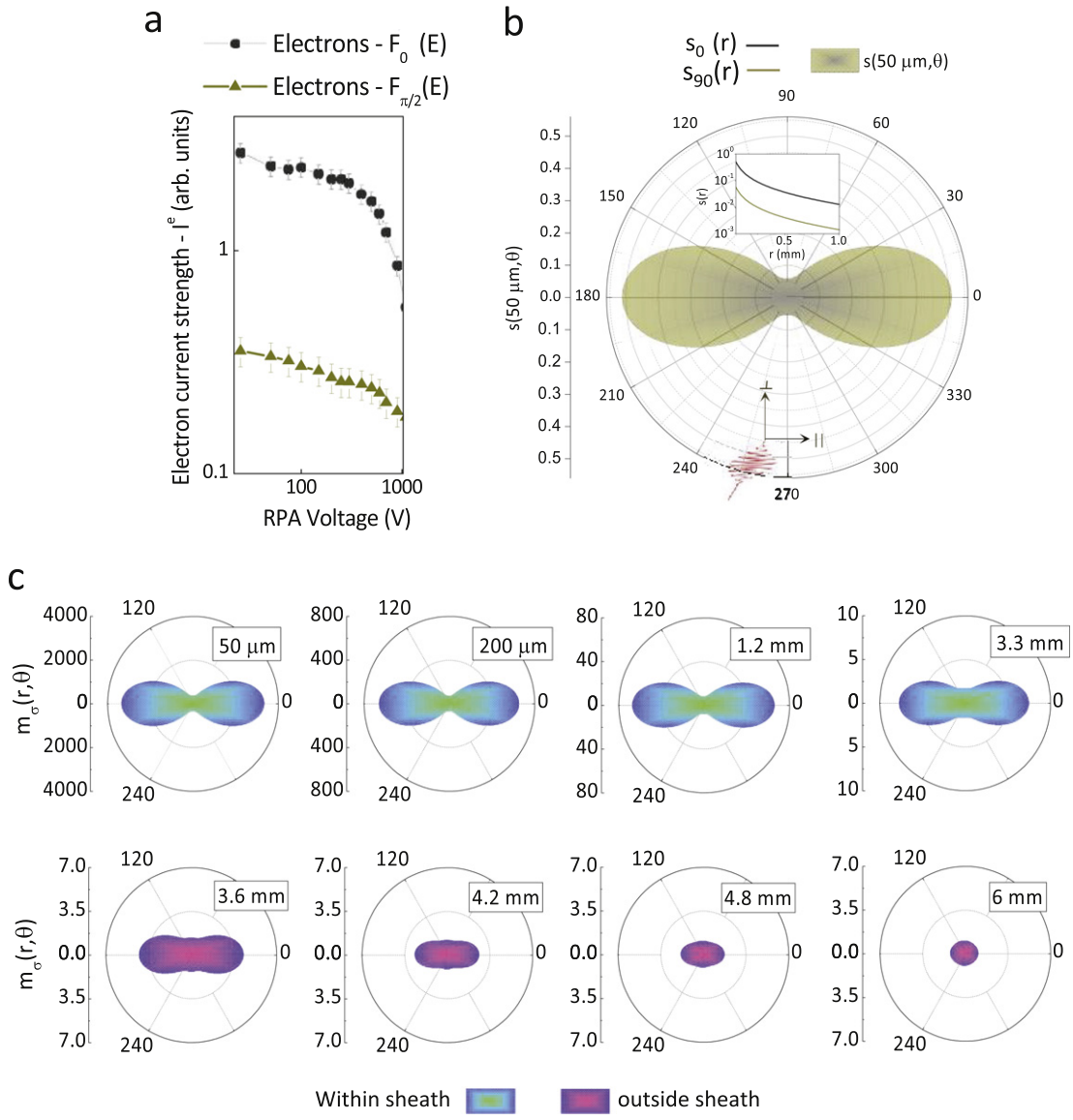

Figure 4. (a) Electron spectra measured using a repellar plate analyzer (RPA) in the parallel (0) and perpendicular ($\pi/2$) directions show a nine times larger electron flux along the laser polarization. (b) Inelastic collisions excite a fraction of clusters to Rydberg states and the inset shows the radial variation of the computed excited cluster fraction (s) within the gas jet (r) for the two polarizations. A polar plot of the $s\,(r,\,\theta)$, at $r = 50\mu$m is also shown to illustrate the angular distribution. (c) Angular dependence of the enhancement in effective cross section $m_\sigma\,(r,\,\theta)$ (see equation (3)) due to the Rydberg excited cluster sheath is computed for various radial distances r from the focus. At distances closer to the laser focus (blue-green plots), a very anisotropic and large excited cluster fraction gives a strongly anisotropic and highly enhanced effective charge transfer cross section. Far away from the laser focus (red-violet plots), s is very small and the isotropic normal charge transfer is effective.

excited cluster sheath along the polarization direction. A self-consistent neutralization model detailed below translates this ratio κ into a neutral yield ratio y^{N} close to the measured value of 1.5.

To compute the neutralization yield as a function of the polarization direction, we use the recent formalism in [15]. Briefly, an ion formed at the laser focus undergoes charge transfer collisions with electrons or clusters as it traverses the supersonic jet before reaching the detector. The capture of a free electron has much smaller cross section and makes negligible contribution to neutralization compared to the capture of a bound electron from clusters in ground state via a normal collisional charge transfer mechanism. Charge transfer cross section from an excited system, on the other hand, is much larger. The capture cross section scales as $\langle n^{\star}\rangle^4$ [17], where $\langle n^{\star}\rangle$ is the effective principle quantum number of the excited target in the collision. Electrons emitted from the laser focus move ahead of the ions and electronically excite some fraction of the clusters [16]. Ions are reduced to neutrals by the enhanced charge transfer from Rydberg excited clusters (ECTREC). The charge transfer physics has also been shown to comprehend well the charge reduction for the different charge states produced in these clusters [33]. In these experiments the ionization of isolated Ar clusters is shown to produce a wide charge distribution with Ar^{8+} as the most dominant ion and a mean charge of 7.6. At a more modest cluster ensemble

density (5×10^{12} W cm^{-3}), the charge reduction by ECTREC to neutrals is not complete but the charge propensity distribution shifts drastically to low charge states. The mean charge is shown to reduce from 7.6 to 2.8 where Ar^{2+} becomes the most dominant with the same energy as that of the highly charged ions. Our ECTREC formalism has been shown to reproduce well the charge histograms that are experimentally measured by accounting for the charge state dependent charge transfer rates [33].

Using the experimentally measured nine-fold larger electron emission along the laser polarization, and a recent result which shows that electron yield varies with the angle of polarization as $\cos^4(\theta)$ in clusters [34] (θ is the angle between the plane of polarization and electron emission direction), the dependence of the fraction of excited clusters formed is obtained as

$$s(r, \theta) = \left[(1 - \kappa)\cos^4(\theta) + \kappa\right] s(r) \tag{3}$$

where $s(r)$, the fraction of excited clusters at a distance r from the laser focus, is computed by evaluating the collisional rate of electron energy loss [23]. Figure 4(b) shows a polar plot of the computed angular distribution of $s(r, \theta)$ at a radial distance of $r = 50$ μm, using the known collisional excitation cross sections [35] for the measured cluster density and the spatial extent of the supersonic jet [36]. The inset shows the radial function of $s(r)$ for the parallel and perpendicular directions. Since the excited cluster fraction is anisotropic, the dominant charge transfer with excited states is also anisotropic with the polarization angle. The effective charge transfer cross section (σ_{eff}) is scaled with the known charge transfer cross sections of the ground state system (σ_{gnd}) [37] as:

$$\sigma_{\text{eff}}(r, \theta) = \left[1 + s(r, \theta)\left\langle n^{*4}\right\rangle\right]\sigma_{\text{gnd}} \tag{4}$$

The angular dependence of the enhancement in the charge transfer defined as $m_\sigma(r, \theta) = \sigma_{\text{eff}}(r, \theta)/\sigma_{\text{gnd}}$ at various radial distances is given as polar plots in figure 4(c). We use $\langle n^* \rangle$ to be 9, as deduced in previous work [15]. At distances very close to the laser focus (violet colour plots in figure 4(c)), where $s(r)$ is large and $m_\sigma(r, \theta)$ is larger, the sheath is very effective and is highly anisotropic compared to distances far from the laser focus where isotropic normal charge transfer is significant (green colour plots). Using $\sigma_{\text{eff}}(r, \theta)$, charge transfer rates are computed with the measured cluster densities and spatial extent of the supersonic jet [36]. The neutralization yield $Y(r, \theta)$ which is the percentage ratio of the number of neutral atoms generated to that of the number of ions formed in the laser focus is shown in figure 5(a) at several distances from the laser focus. The yield at the end of the supersonic jet (10 mm), which is measured in the experiments, is also shown. The measured neutral atom yield of about 50% at the perpendicular directions and the 90% neutral atom yield along the direction of polarization compares very well with the calculations in figure 5(a). The experimentally determined yield ratio between parallel and perpendicular directions y_{N} is 1.5 and agrees well with 1.7 computed by the model. Close to the laser focus, the charge transfer is essentially due to ECTREC and the anisotropy is very large. Along the laser polarization, the neutralization yield is nearly complete within a traversal of about 25 μm and cannot increase further. In the perpendicular direction, the electronic sheath is much less effective and yield is very small near the laser focus. The normal charge transfer, which is isotropic (indicated as a dotted circle in figure 5(a)) greatly contributes to the 50% neutralization yield observed in experiments. So the anisotropy as measured in the experiment($y^{\text{N}} \sim 1.5$) is smaller than what it would be close to the laser focus.

Apart from the neutralisation yield, we can also compute the the fast atom flux distribution at a given radius r and angle θ as $J^{\text{N}}(r, \theta) = Y(r, \theta) \times J^{\text{I}}(r = r_{\text{source}}, \theta)$. Using the known feature that the angular dependence of an ion source has a $cos^2(\theta)$ dependence [21], the fast atom flux distribution at the jet end is computed as shown in figure 5(b) along with the ion source flux distribution. The neutral atom distribution is very directional at the end of the excited cluster sheath ($r < 250$ μm) and is more directional than ions even at the end of the jet. Clearly the sheath anisotropy gives anisotropy for fast atoms. The blue line in figure 5(b) corresponds to the case of neutral emission sans the sheath.

The neutral yield measurement thus demonstrates that the sheath of Rydberg excited clusters is anisotropic. The density of Rydberg excited clusters along the direction of polarization is about 8–9 times larger. Thus electron anisotropy not only drives ion anisotropy but also enhanced neutral atom anisotropy. It is possible to change the transverse modes of the laser beam that can alter the electron energy distribution and in turn the neutral atom distribution. Optimizing the laser parameters can result in a more directed emission of high energy neutrals with appropriate ($\simeq$30 keV) average energy which would be very crucial for applications in lithography and tokomak diagnostics. The results presented here show that charge transfer in cluster plasmas is not a passive mechanism. Manipulating the Rydberg excited states demonstrated here has implications in most laser produced plasmas and could be crucial for many novel application schemes.

In summary, we demonstrate polarization dependent anisotropy in neutralization, which the Coulomb exploded ions undergo in intense laser fields. Neutral atom emission is three times larger along the direction of

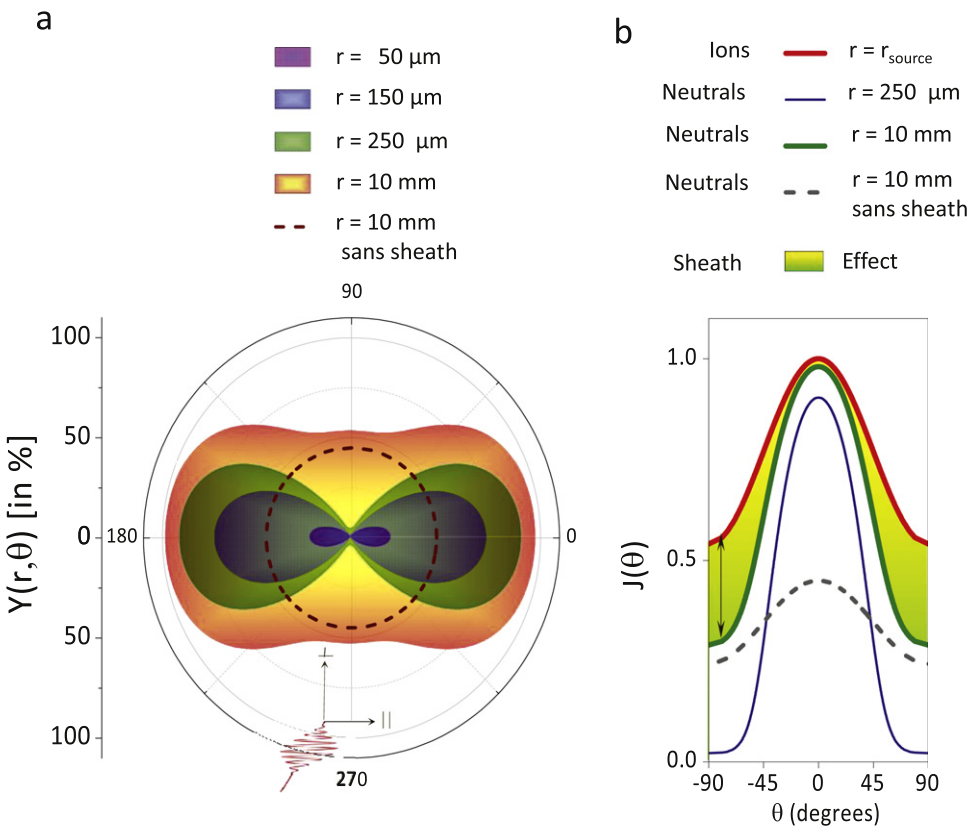

Figure 5. (a) Polar plot of the computed neutralization yield (percentage of atoms neutralized) due to the enhanced charge transfer by Rydberg excited clusters [15] at different distances from the laser focus. The curve at 10 mm is the neutralization yield expected at the end of the jet in experiments. The dotted line represents the isotropic neutralization due to normal charge transfer sans Rydberg excited sheath. (b) The normalized emission flux for ions and neutrals $J(\theta)$ computed at the end of the jet. Neutral emission has narrower angular distribution due to the anisotropic sheath effect.

light polarization and is much larger than that of ions. The additional anisotropy is due to the relatively larger efficacy of the enhanced charge transfer by Rydberg excited clusters that are anisotropically generated. We measure the anisotropy in electron emission and use it to compute the formation of a larger density of Rydberg excited clusters along the laser polarization direction. Larger charge transfer rate along the polarization is computed to comprehend the preferential emission of neutrals along the laser polarization. The computed neutral atom anisotropy compares well with the measurements. This work demonstrates that charge transfer reaction in laser produced plasma can be actively influenced by laser polarization via the electron emission propensity. Any change in laser parameters that influences the electron emission will affect the Rydberg excited sheath and in turn have a direct impact on the charge composition of the ions or the neutral atom emission characteristics.

Acknowledgments

MK acknowledges Swarnajayanti Fellowship from the Department of Science and Technology, Government of India.

References

[1] Malka V *et al* 2008 *Nat. Phys.* **4** 447–53
[2] Esarey E, Schroeder C B and Leemans W P 2009 *Rev. Mod. Phys.* **81** 1229
[3] Sarri G *et al* 2013 *Phys. Rev. Lett* **110**
[4] Hegelich B M *et al* 2006 *Nature* **439** 441–4
[5] Maksimchuk A *et al* 2000 *Phys. Rev. Lett.* **84** 4108
[6] Brabec T and Krausz F 2000 *Rev. Mod. Phys.* **72** 545
[7] Saalmann U, Siedschlag Ch and Rost J M J 2006 *Physica* B **39** R39
[8] Krainov V P and Smirnov M B 2002 *Phys. Rep.* **370** 237
[9] Rajeev R *et al* 2011 *Rev. Sci. Instrum.* **82** 083303
[10] Ditmire T *et al* 1998 *Phys. Rev.* A **57** 369

[11] Amiranoff F 1998 *Phys. Rev. Lett.* **81** 995
[12] Margarone D *et al* 2012 *Phys. Rev. Lett.* **109** 234801
[13] Kim H T *et al* 2013 *Phys. Rev. Lett.* **111** 165002
[14] Williams G O *et al* 2009 *Appl. Phys. Lett.* **94** 101503
[15] Rajeev R *et al* 2013 *Nat. Phys.* **9** 185
[16] Rajeev R *et al* 2013 *Phys. Plasmas* **20** 120701
[17] Harth K, Ruf M W and Hotop H 1989 *Z. Phys.* D **14** 149–65
[18] Wolfe J C and Craver B P 2008 *J. Phys. D: Appl. Phys.* **41** 024007
[19] Saravia E, Castracane J and Woo J T 1990 *Rev. Sci. Instrum.* **61** 3528–31
[20] Huismans Y *et al* 2011 *Science* **331** 61
[21] Kumarappan V, Krishnamurthy M and Mathur D 2003 *Phys. Rev.* A **67** 043204
[22] Jha J and Krishnamurthy M 2008 *J. Phys. B: At. Mol. Opt. Phys.* **41** 41002
[23] Rajeev R *et al* 2013 *Phys. Rev.* A **87** 053201
[24] Zherebtsov S *et al* 2011 *Nat. Phys.* **7** 656
[25] Kumarappan V, Krishnamurthy M and Mathur D 2001 *Phys. Rev. Lett.* **87** 085005
[26] Jungreuthmayer C *et al* 2004 *Phys. Rev. Lett.* **92** 133401
[27] Skopalova E *et al* 2012 *Phys. Rev. Lett.* **104** 203401
[28] Hagena O F 1987 *Z. Phys.* D **4** 291
[29] Kumarappan V *et al* 2001 *Phys. Rev.* A **63** 023203
[30] Gao X *et al* 2012 *Appl. Phys. Lett.* **100** 064101
[31] Jha J and Krishnamurthy M 2009 *Phys. Rev.* A **80** 043202
[32] Ranaul Islam Md, Saalmann U and Rost J M 2006 *Phys. Rev.* A **73** 041201(R)
[33] Madhu Trivikram T, Rajeev R, Rishad K P M, Jha J and Krishnamurthy M 2013 *Phys. Rev. Lett.* **111** 143401
[34] Passig J *et al* 2012 *New J. Phys.* **14** 085020
[35] Raju G 2004 *IEEE Trans. Dielectr. Electr. Insul.* **11** 649–73
[36] Rajeev R *et al* 2013 *J. Appl. Phys.* **114** 083112
[37] Vancura J *et al* 1994 *Phys. Rev.* A **49** 2515–23